Ear, Nose & Throat Journal
1–9

DOI: 10.1177/01455613251335109
journals.sagepub.com/home/ear
Sage

Computational Modeling of Nasal Cavity Aerodynamics: Implications for Surgical Outcomes and Targeted Drug Administration

Guiliang Liu, BS[1], W. Jared Martin, BA[2], Yasine Mirmozaffari, BS[2], Rui Ni, PhD[3], and Zheng Li, PhD[1]

Abstract

The primary goal of sinonasal surgery is to improve a patient's quality of life, which is generally achieved by enhancing drug delivery (eg, saline rinses, nasal steroids) and nasal airflow. Both drug delivery and nasal airflow are dependent on the anatomic structure of the sinonasal cavity and the relationship between this anatomy and airflow and drug delivery can be studied using computational fluid dynamics (CFD). CFD generally uses computed tomography scans and computational algorithms to predict airflow or drug delivery and can help us understand surgical outcomes and optimize drug delivery for patients. This study employs CFD to simulate nasal airflow dynamics and optimize drug delivery in the nasal cavity to highlight the utility of CFD for studying sinonasal disease. Utilizing COMSOL Multiphysics software, we developed detailed models to analyze changes in airflow characteristics before and after functional endoscopic sinus surgery, focusing on pressure distribution, velocity profiles, streamline patterns, and heat transfer. This research examines the impact of varying levels of nasal airway obstruction on airflow and heat transfer. In addition, we explore the characteristics of nasal drug delivery by simulating diverse spray parameters, including particle size, spray angle, and velocity. Our comprehensive approach allows for the visualization of drug particle trajectories and deposition patterns, providing crucial insights for enhancing surgical outcomes and improving targeted drug administration. By integrating patient-specific nasal cavity models and considering factors such as airway outlet pressure, this study offers valuable data on pressure cross-sections, flow rate variations, and particle behavior within the nasal passages. The findings of this research can be useful for both surgical planning and the development of more effective nasal drug delivery methods, potentially leading to enhanced clinical outcomes in respiratory treatment.

Keywords

nasal cavity flow, drug delivery, numerical simulation, pressure and velocity distributions

Introduction

The human nasal cavity plays a crucial role in respiratory function, serving as the primary conduit for airflow and acting as a first line of defense against airborne particles and pathogens. Its complex anatomy, characterized by intricate turbinate structures and narrow passageways, significantly influences airflow dynamics and particle deposition patterns. In recent years, there has been a growing interest in understanding and optimizing nasal airflow, both for improving surgical outcomes in otolaryngology and enhancing the efficacy of intranasal drug delivery systems.[1-3]

Sinonasal surgeries, such as septoplasty, turbinate reduction, and functional endoscopic sinus surgery (FESS)

[1]Mechatronics Engineering, Morgan State University, Baltimore, MD, USA
[2]Department of Otolaryngology-Head & Neck Surgery, University of North Carolina at Chapel Hill, NC, USA
[3]Department of Mechanical Engineering, Johns Hopkins University, Baltimore, MD, USA

Zheng Li is also affiliated with Department of Otolaryngology-Head & Neck Surgery, University of North Carolina at Chapel Hill, NC, USA

Received: February 12, 2025; revised: March 11, 2025; accepted: March 17, 2025

Corresponding Author:
Zheng Li, PhD, Morgan State University, 1700 E Cold Spring Ln, Baltimore, MD 21251-0001, USA.
Email: Zheng.li@morgn.edu

procedures, are commonly performed to alleviate nasal congestion and sinus disease, respectively. While the primary goal of sinonasal surgery is to improve a patient's quality of life, this is generally achieved by improving drug delivery (saline rinses, nasal steroids) and nasal airflow. While this airflow is related to the radius of the airway, this relationship is more complex within the anatomy of the nasal cavity. In addition, different medical treatments likely should be targeted to different anatomic locations within the sinonasal tract (ie, allergic rhinitis—inferior turbinate, nasal polyps—sinus cavity, olfactory dysfunction—olfactory cleft). Despite understanding where therapeutics may provide the most benefit, it is not well known how we can deliver them to distinct anatomic targets.[4-7]

In light of these challenges, numerical simulations and computational fluid dynamics (CFD) have emerged as powerful tools for investigating nasal airflow and drug delivery. CFD uses numerical analysis and algorithms to solve and analyze problems involving fluid (including air) flows. It simulates the behavior of liquids and gases by solving complex mathematical equations (eg, Navier–Stokes equations) that describe fluid motion. When related to the sinonasal cavity, CFD generally utilizes a computed tomography (CT) scan to construct the relevant anatomy and Ansys (ANSYS, Canonsburg, PA, USA) or COMSOL Multiphysics (COMSOL Inc., Burlington, MA, USA) can be used to model predicted airflow and drug delivery.

These computational methods offer several advantages over traditional experimental approaches, including the ability to provide detailed, noninvasive visualizations of airflow patterns and particle trajectories within patient-specific nasal geometries.[8-10] By leveraging advanced software such as COMSOL Multiphysics (COMSOL Inc. Burlington, MA, USA), researchers can now create highly detailed models that account for the intricate anatomical features of the nasal cavity and simulate a wide range of physiological conditions and drug delivery scenarios.[11,12]

CFD for Sinonasal Airflow

Lu et al[13] conducted a rigorous validation study of CFD models for nasal airflow. Their research, involving 10 subjects with normal nasal cavities, utilized CT scans, acoustic rhinometry, and rhinomanometry to create and validate 3-dimensional (3D) models. The study confirmed the accuracy of CFD simulations in replicating nasal airflow characteristics, particularly in capturing laminar flow patterns and pressure distributions throughout the nasal cavity.

Calmet et al[14] further expanded on these findings by comparing various CFD methodologies for simulating nasal airflow under diverse conditions. Their study evaluated laminar models, Reynolds-averaged Navier–Stokes (RANS) turbulence models, large eddy simulation (LES), and direct numerical simulation (DNS) using an anatomically accurate nasal model. Results indicated that while laminar models suffice for restful breathing, more sophisticated approaches like LES and DNS offer superior accuracy across a broader range of conditions, albeit with increased computational demands.

These studies collectively demonstrate the potential of numerical simulations to inform surgical planning and enhance drug delivery strategies in otolaryngology, providing a foundation for further research and clinical applications in this field. Croce et al[15] conducted a comprehensive study comparing in vitro experiments with CFD simulations to analyze pressure-flow relationships in human nasal cavities and maxillary sinuses. Their research compared plastinated human nasal specimens to 3D reconstructions from CT scans, tested flow rates up to 1500 ml/second using various gases under in vitro conditions, and simulated inspiratory airflow up to 353 ml/second using CFD. The study demonstrated congruence between measured and simulated pressure drops up to 250 ml/second, validating the CFD software's capability to model physiologically realistic nasal airflow. Key findings revealed that the nasal valve region is the primary site of pressure drop, with airflow predominantly occurring in the inferior medial region of the nasal cavities.

Van Strien et al[16] conducted a comprehensive study on nasal cavity fluid dynamics using time-dependent CFD simulations. Employing a hybrid RANS-LES model, they examined inhalation at flow rates ranging from 10 to 30 l/minute. The study revealed significant pressure drops at the level of the nasal valve and nasopharynx due to narrow cross-sectional areas at these anatomical sites. At higher flow rates (30 l/minute), disturbed laminar flow was observed in the anterior nasal cavity, with turbulent activity observed in the posterior region. Conversely, lower flow rates (15 l/minute) exhibited predominantly laminar flow throughout the nasal tract.

Tretiakow et al[17] aimed to develop a comprehensive workflow for conducting CFD simulations of airflow through the upper airways based on CT and cone-beam computed tomography (CBCT) images of individual adult patients. The research utilized CT images from 16 patients to create 3D models of the nasal cavity and paranasal sinuses using open-source and freeware software, primarily 3D Slicer for segmentation and Autodesk® Meshmixer™ (Autodesk, Inc. San Francisco, CA, USA) for further processing. The finite volume method was employed to discretize the governing equations, which were then solved using OpenFOAM software (open-source software which is freely available and licensed under the GNU General Public License). The study detailed the protocol for preparing 3D models and highlighted potential challenges for future researchers. CFD results were demonstrated using models from 2 patients, 1 with normal anatomy, and 1 with pathological changes. This study emphasized the short training time required for users without prior experience in image segmentation and 3D mesh editing and noted that while both CBCT and CT are useful for model building, CBCT may be more limited.

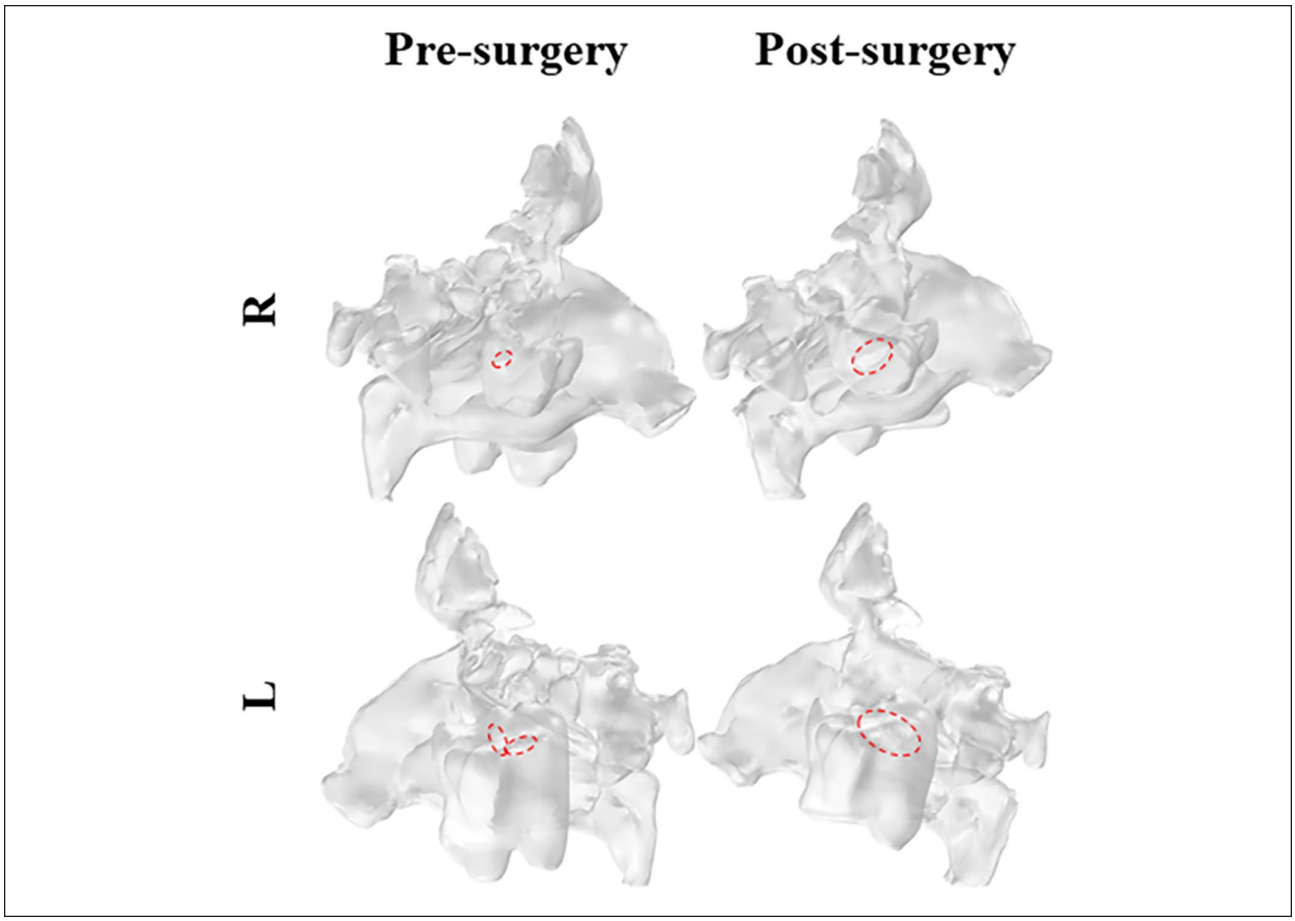

Figure 1. The nasal cavity system of a patient before and after surgery is depicted. The red circles show the entrance of sinuses which play an important role in breathing control.

Study Objectives

In this study, we aim to leverage advanced numerical simulation techniques to comprehensively analyze nasal airflow dynamics and optimize drug delivery strategies. Our primary objectives are 3-fold: First, we will investigate the pressure distribution, velocity changes, and streamline patterns of nasal airflow pre- and post-surgery, with particular emphasis on identifying newly accessible airflow regions following surgical intervention. Second, we will examine airflow characteristics under various breathing pressures, including scenarios of increased nasal airway obstruction, to observe changes in turbulence and streamline patterns. Finally, we will develop a COMSOL Multiphysics-based numerical simulation model for nasal spray delivery, enabling detailed visualization of drug particle trajectories and deposition patterns under different spray parameters and orientations. Through this multifaceted approach, we seek to provide valuable insights that can inform surgical planning, enhance postoperative care, and improve the efficacy of intranasal drug delivery systems. The findings of this study have the potential to contribute to the fields of otolaryngology and pharmaceutical sciences, ultimately leading to improved patient outcomes and more targeted therapeutic strategies.

Problem Description

Preoperative surgical and postoperative surgical scans are used to generate a 3D reconstruction of the airspace (Figure 1). Post-surgical scans can be generated using virtual surgery, dicom exports from select navigation systems, or actual post-surgical CT scans. The red circles indicate the sinus entrances that have been enlarged following surgery. These specifically represent the maxillary sinus ostium, which has been widened through FESS to facilitate improved sinus ventilation and drainage. These pre- and post-surgical scans can be used to define pressure, streamlines, and velocity to understand the effects of surgery on changes in the sinonasal cavity in a holistic manner.

Mathematical Modeling

The flow in the nasal cavity is considered to be 3D, unsteady, incompressible, laminar, and isothermal.

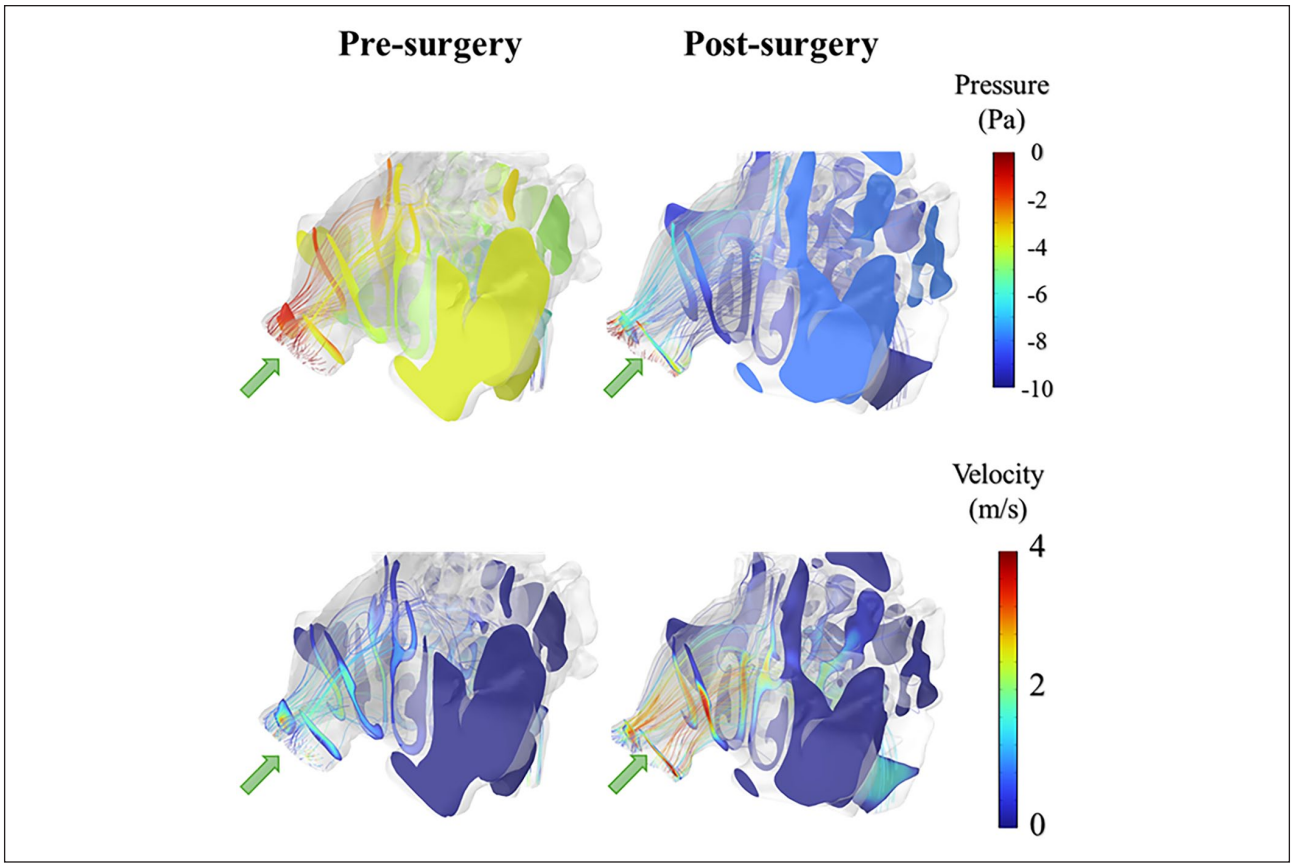

Figure 2. Pressure (top) and velocity distributions (bottom) within the nasal cavity for the pre- and post-surgery.

Governing Equations

The continuity equation for such a flow can be described as[18]:

$$\nabla.\left(\vec{u}\right)=0 \tag{1}$$

where $\vec{u}$ is the 3D velocity field. The momentum conservation (Navier–Stocks) equations can be written as[18]:

$$\rho\left(\vec{u}.\nabla\right)\vec{u}=-\nabla p+\mu\nabla^2\vec{u} \tag{2}$$

Here, ρ is the density of air $(=1\mathrm{kg}/\mathrm{m}^3)$, p is the pressure field (Pa), and μ is the viscosity of air $(=1.81\times10^{-5}\,\mathrm{kg}/\mathrm{m.s})$.[19] The Reynolds number will be decided by the pressure difference and geometry of the nasal cavity, which is around 2000. In this work, we tested both laminar model and turbulent model while the airflow, heat transfer, and drug delivery do not show significant differences.

Results and Discussions

Airflow Improvement From Surgery

Preoperative analysis revealed substantial regions of elevated pressure (denoted by warmer colors, yellow, orange, and red) accompanied by zones of low airflow velocity (indicated in dark blue; Figure 2). These findings highlight severe airflow obstruction in the nasal passages, resulting in significant aerodynamic resistance. Post-FESS, the cross-sectional models of airflow pressure and velocity reveal a pressure reduction and velocity increase (Figure 2). These airflow improvements primarily stem from the enlarged maxillary sinus ostium, which substantially reduces airflow resistance at the sinus entrance. The surgical intervention effectively augmented the cross-sectional area of the nasal passages, as evidenced by the more uniform pressure gradients and improved flow characteristics. Moreover, the postoperative state exhibited enhanced streamlined continuity and stability, quantitatively confirming the reduction in nasal airway resistance and the establishment of more homogeneous airflow patterns throughout the nasal cavity.

The 3D visualization of pressure distribution and velocity streamlines within the nasal cavity system revealed significant differences before and after surgical intervention (Figures 3 and 4). Preoperative streamline patterns showed pronounced flow restrictions throughout the nasal cavity, particularly in the middle and posterior regions, characterized by flow stagnation and

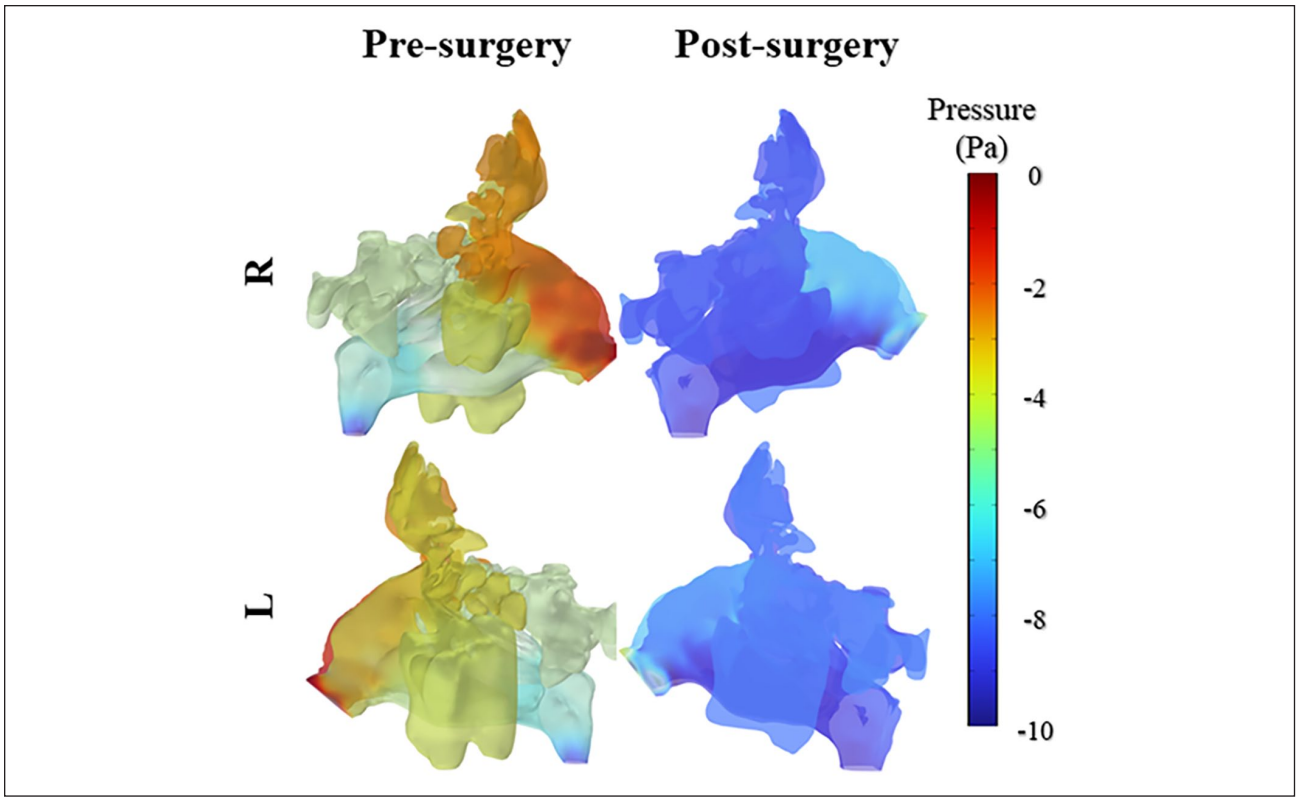

Figure 3. 3D view of pressure distribution inside the nasal cavity of the patient before and after surgery. 3D, 3-dimensional.

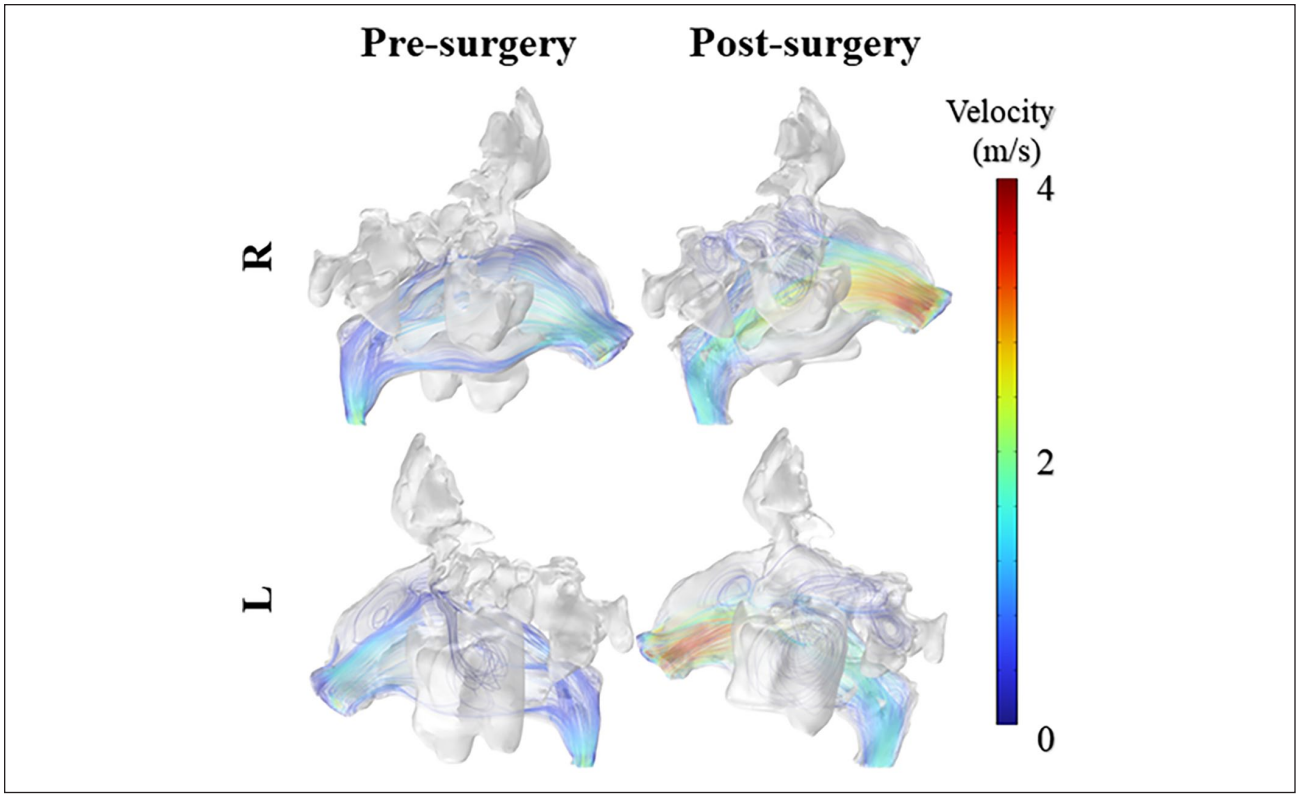

Figure 4. Streamlines and velocity magnitudes within the nasal cavity before and after surgery in a 3D view. 3D, 3-dimensional.

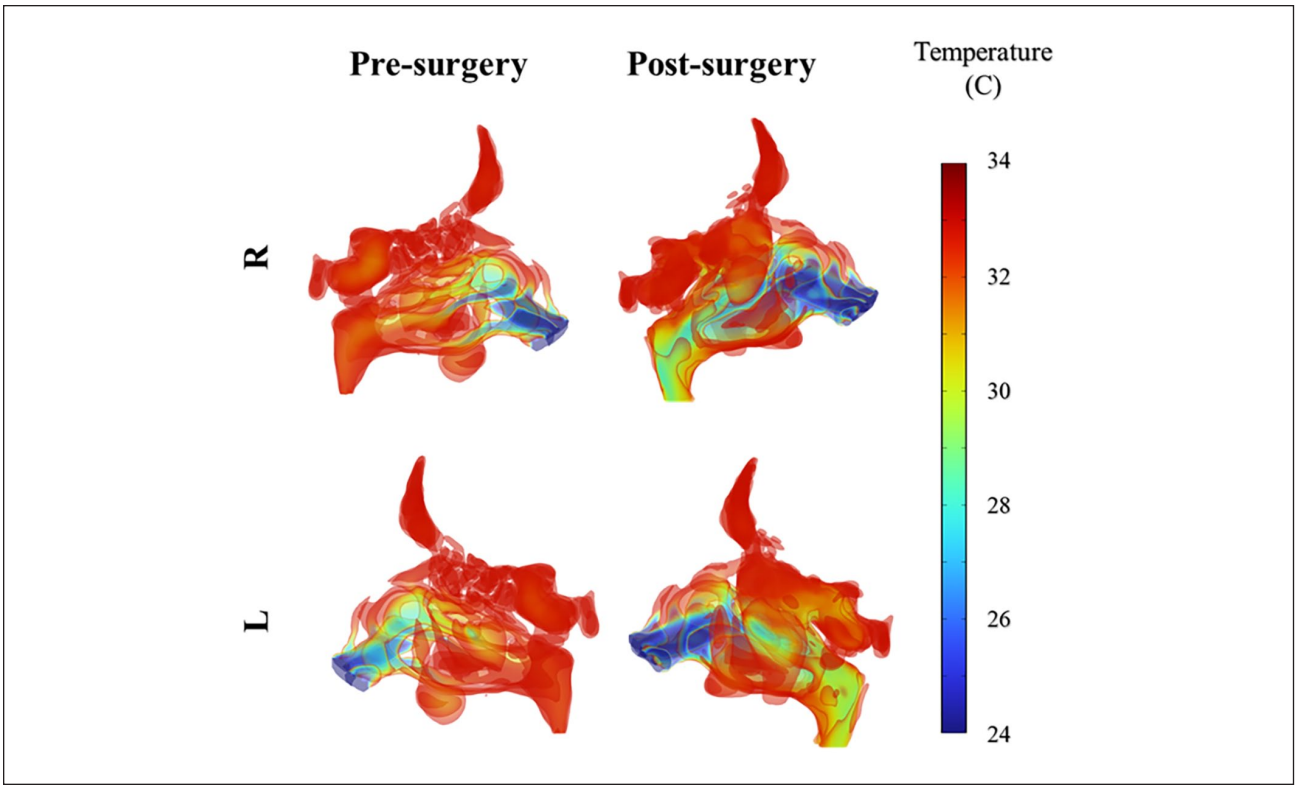

Figure 5. Temperature distribution within the right (R) and left (L) parts of the nasal cavity after and before surgery.

low-velocity zones. By contrast, postoperative streamline patterns demonstrated markedly improved flow characteristics, with more continuous and uniform patterns, especially near the sinus ostia. This improvement was evidenced by the transition in streamlined colors from blue to yellow and red, reflecting a substantial increase in local flow velocities.

The pressure distribution analysis further corroborates these improvements, showing that the preoperative state was characterized by high-pressure regions that impeded airflow, particularly in the constricted superior and middle portions of the nasal cavity. Postoperatively, these high-pressure zones were significantly alleviated, resulting in a more homogeneous pressure distribution throughout the nasal passages. The comparative analysis of both pressure and velocity distributions provides compelling evidence that the surgical intervention successfully reduced airway resistance, leading to enhanced airflow dynamics and improved ventilation efficiency within the nasal cavity system. These improvements suggest better physiological functioning of the nasal airways, potentially contributing to enhanced patient comfort and respiratory performance.

Thermal Transportation Improvement From Surgery

While clinically most of our surgeries are designed to reduce perceived pressure in the sinonasal cavity and improve airflow, mechanistically the improved sensation is thought to come from changes in heat flux on the mucosal surfaces. The increased airflow is to be sensed through increased heat flux due to the cooling effects of airflow. Analysis of the pre- and post-surgical thermal distribution patterns demonstrates that surgical intervention resulted in lower temperatures (as indicated by cooler colors) throughout the nasal cavity, suggesting enhanced airflow (Figure 5). Preoperatively, the nasal airflow exhibited significant constriction, characterized by heterogeneous distribution and regions of diminished velocity, particularly proximal to the turbinates and cavity floor. These zones demonstrated inadequate airflow mechanics and restricted thermal exchange, yielding localized thermal readings substantially above the physiological nasal mucosal temperature of 32°C. The flow characteristics displayed notable irregularities, with evident turbulent structures and vortical

formations, compromising aerodynamic efficiency and generating regions of minimal air circulation. Moreover, the incoming airstream at 24°C demonstrated insufficient thermal conditioning across the nasal passages due to discontinuous flow trajectories, potentially compromising respiratory comfort and physiological air-conditioning function.

Post-surgical intervention, the anatomical optimization of the nasal cavity yielded substantial improvements in flow dynamics. The airflow patterns demonstrated enhanced uniformity, with elevated velocities in previously constricted regions and a marked reduction in turbulent structures. The flow streamlines exhibited increased regularity and continuity, facilitating airflow penetration into previously inaccessible nasal regions. The thermal distribution analysis revealed significant enhancement, with the majority of regions approaching the physiological mucosal temperature of 32°C, indicating superior heat transfer efficiency. The reduced airway resistance and improved flow distribution suggest optimization of both aerodynamic performance and respiratory function, potentially enhancing patient comfort and the physiological air-conditioning capacity of the nasal cavity.

Drug Delivery Improvement From Surgery

CFD can be used to simulate nasal drug delivery. The CFD model utilized in this study revealed how the spatial distribution of particle deposition within the nasal cavity is influenced by the position and directional configuration of the intranasal spray tip (Figure 6a). Furthermore, it demonstrates how particle size characteristics affect their distribution patterns, based on a logarithmic distribution[18] (Figure 6b). By utilizing COSMOL Multiphysics, a computation model was developed to demonstrate the predicted shape and pattern of a typical spray (Figure 6c).

This spray model enabled the creation of a quantitative comparison to predict the drug particle mass fraction deposition in the ostiomeatal complex based on spray angles (50° and 25°) and the nasal passage used (left vs right; Figure 6d). In this study, we specifically examined spray angles of 25° and 50°. The 25° angle was selected as it represents the actual spray angle utilized in a commercially available nasal spray device. The 50° angle, representing twice the width of the standard angle, was chosen as a comparative parameter to evaluate how broader spray dispersion affects drug delivery patterns. These 2 distinct angles enable us to systematically assess the impact of spray trajectory on drug deposition efficiency within the nasal cavity. The comparative analysis demonstrates that spray angle orientation substantially influences particle delivery efficacy, with the 25° configuration yielding markedly enhanced particle deposition compared to the 50° orientation. This enhanced performance can be attributed to the improved alignment between the spray trajectory and the anatomical architecture of the nasal cavity at the decreased angle, minimizing off-target particle deposition.

Furthermore, the analysis reveals significant bilateral asymmetry in delivery efficiency between the nasal passages, with the right cavity demonstrating superior particle deposition characteristics. This bilateral variation may be attributed to congenital anatomical asymmetry and consequent differences in local flow dynamics. Among the investigated parameters, optimal particle deposition was achieved with the 25° spray angle configuration in the right nasal passage, suggesting the potential advantages of this specific delivery orientation.

These findings underscore the critical importance of both spray angle optimization and anatomical considerations in determining regional particle deposition patterns, offering valuable insights for the development of patient-specific nasal drug delivery protocols.

Conclusions

In conclusion, clinically relevant rhinologic questions can be addressed using CFD. This study employed COMSOL Multiphysics numerical simulation software to conduct a comprehensive analysis of nasal airflow dynamics before and after surgical intervention, with particular emphasis on respiratory resistance modification and thermal transportation improvement. The comparative analysis of preoperative and postoperative pressure and velocity distributions demonstrated significant improvements in nasal cavity airflow characteristics. These enhancements were particularly pronounced at the sinus ostia, characterized by more uniform flow patterns, reduced pressure gradients, and increased airflow velocities.

Under identical outlet pressure conditions, the effects of FESS facilitated enhanced air entry into the respiratory tract, resulting in reduced breathing resistance and improved respiratory efficiency, which also lead to a valid heat transfer enhancement.

We also highlight the utility of CFD to model COMSOL Multiphysics software to simulate drug spray particle dynamics under various parametric conditions, enabling detailed visualization of drug delivery patterns. This computational model serves as a valuable tool for investigating drug delivery efficiency across different nasal anatomy and flow conditions, providing crucial insights for the

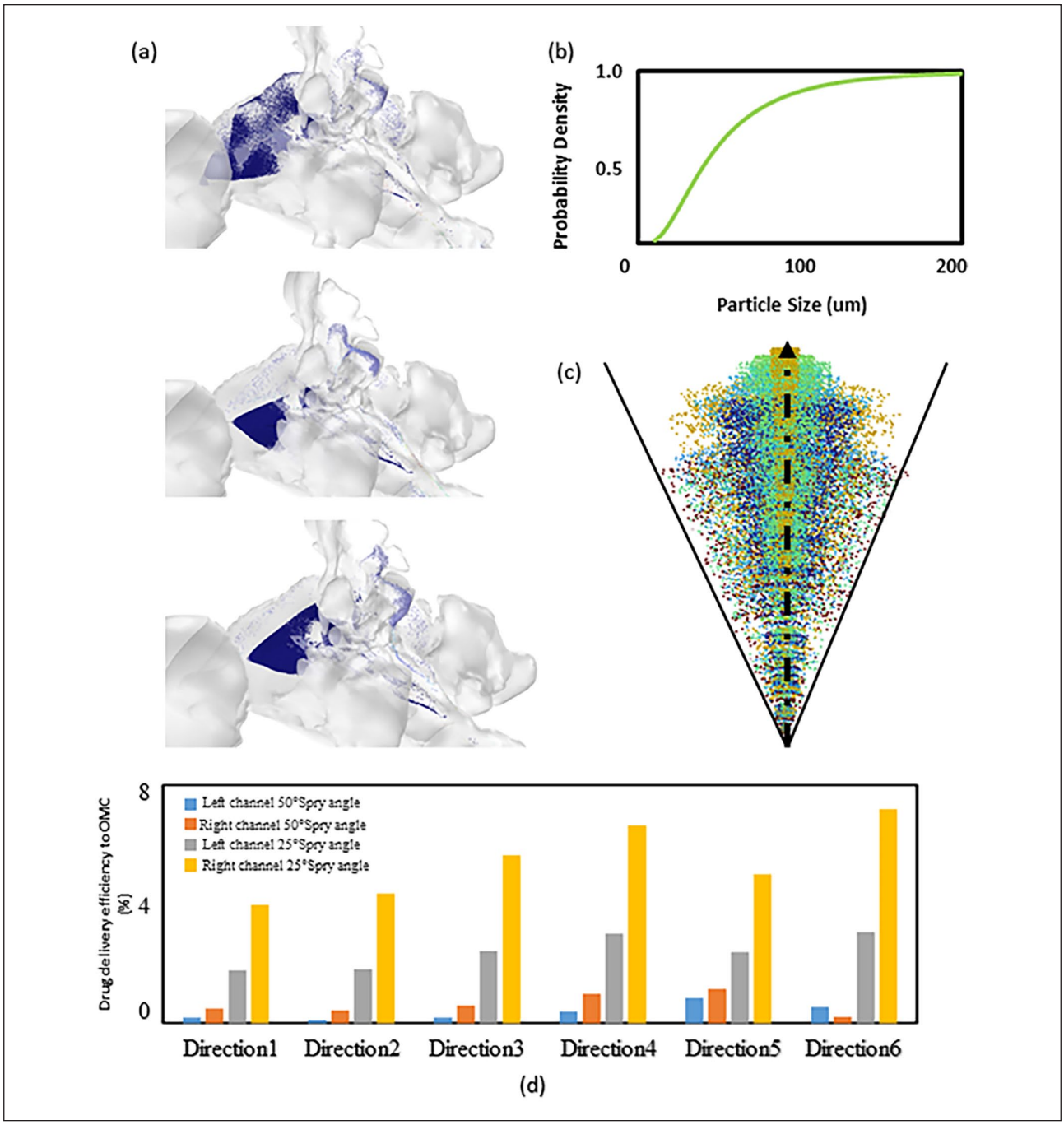

Figure 6. (a) The distribution of particles within the nasal cavity for different injection positions and directional configurations, (b) particle size distribution, (c) computational spray model simulated in COMSOL Multiphysics, and (d) drug particle mass fraction deposition in the OMC region at different spray angles (50° and 25°). OMC, ostiomeatal complex.

optimization of clinical spray treatments. The findings presented in this study offer substantive scientific evidence for both the evaluation of surgical outcomes and the refinement of therapeutic drug delivery strategies in nasal treatments. These results contribute significantly to the advancement of clinical practice in both surgical intervention and pharmaceutical administration within the nasal cavity system.

ORCID iDs

W. Jared Martin https://orcid.org/0009-0001-9227-4003
Zheng Li https://orcid.org/0000-0002-0132-8812

Funding

The author(s) disclosed receipt of the following financial support for the research, authorship, and/or publication of this article: This work is sponsored by an NSF grant with Award Number: 2401855 and an NIH grant with Award Number: R16GM153629.

Declaration of Conflicting Interests

The author(s) declared no potential conflicts of interest with respect to the research, authorship, and/or publication of this article.

References

1. Borthakur MP, Succi S, Sterpone F, Pérot F, Diko A, Melchionna S. In-silico analysis of airflow dynamics and particle transport within a human nasal cavity. *J Comput Sci*. 2021;54:101411. doi:10.1016/j.jocs.2021.101411
2. Bradshaw K, Warfield-Mcalpine P, Vahaji S, et al. New insights into the breathing physiology from transient respiratory nasal simulation. *Phys Fluids*. 2022;34(11):1-14. doi:10.1063/5.0112223
3. Schroeter JD, Kimbell JS, Asgharian B. Analysis of particle deposition in the turbinate and olfactory regions using a human nasal computational fluid dynamics model. *J Aerosol Med*. 2006;19(3):301-313. doi:10.1089/jam.2006.19.301
4. Ma R, Tian L, Wang Y, et al. Comparative investigation of transport and deposition of nebulized particles in nasal airways following various middle turbinectomy. *Rhinology*. 2024;62(2):223-235. doi:10.4193/Rhin23.265
5. Warnken ZN, Smyth HDC, Davis DA, Weitman S, Kuhn JG, Williams RO III. Personalized medicine in nasal delivery: the use of patient-specific administration parameters to improve nasal drug targeting using 3D-printed nasal replica casts. *Mol Pharm*. 2018;15(4):1392-1402. doi:10.1021/acs.molpharmaceut.7b00702
6. Momeni Larimi M, Babamiri A, Biglarian M, Ramiar A, Tabe R, Inthavong K, Farnoud A. Numerical and experimental analysis of drug inhalation in realistic human upper airway model. *Pharm*. 2023;16(3):406. https://www.mdpi.com/1424-8247/16/3/406
7. Oliveira A, Marques A. Respiratory sounds in healthy people: a systematic review. *Resp Med*. 2014;108(4):550-570. doi:10.1016/j.rmed.2014.01.004
8. Kleven M, Melaaen MC, Reimers M, Røtnes JS, Aurdal L, Djupesland PG. Using computational fluid dynamics (CFD) to improve the bi-directional nasal drug delivery concept. *Food Bioprod Process*. 2005;83(2):107-117. doi:10.1205/fbp.04403
9. Chari S, Sridhar K, Walenga R, Kleinstreuer C. Computational analysis of a 3D mucociliary clearance model predicting nasal drug uptake. *J Aerosol Sci*. 2021;155:105757. doi:10.1016/j.jaerosci.2021.105757
10. Cherobin GB, Voegels RL, Gebrim EMMS, Garcia GJM. Sensitivity of nasal airflow variables computed via computational fluid dynamics to the computed tomography segmentation threshold. *PLoS One*. 2018;13(11):e0207178. doi:10.1371/journal.pone.0207178
11. Farnoud A, Baumann I, Rashidi MM, Schmid O, Gutheil E. Simulation of patient-specific bi-directional pulsating nasal aerosol dispersion and deposition with clockwise 45° and 90° nosepieces. *Comput Biol Med*. 2020;123:103816. doi:10.1016/j.compbiomed.2020.103816
12. Gonda I. Mathematical modeling of deposition and disposition of drugs administered via the nose. *Adv Drug Deliv Rev*. 1998;29(1):179-184. doi:10.1016/S0169-409X(97)00068-9
13. Lu J, Han D, Zhang L. Accuracy evaluation of a numerical simulation model of nasal airflow. *Acta Otolaryngol*. 2014;134(5):513-519. doi:10.3109/00016489.2013.863430
14. Calmet H, Inthavong K, Owen H, et al. Computational modelling of nasal respiratory flow. *Comput Methods Biomech Biomed Eng*. 2021;24(4):440-458. doi:10.1080/10255842.2020.1833865
15. Croce C, Fodil R, Durand M, et al. In vitro experiments and numerical simulations of airflow in realistic nasal airway geometry. *Ann Biomed Eng*. 2006;34(6):997-1007. doi:10.1007/s10439-006-9094-8
16. Van Strien J, Shrestha K, Gabriel S, et al. Pressure distribution and flow dynamics in a nasal airway using a scale resolving simulation. *Phys Fluids*. 2021;33(1):011907. doi:10.1063/5.0036095
17. Tretiakow D, Tesch K, Meyer-Szary J, Markiet K, Skorek A. Three-dimensional modeling and automatic analysis of the human nasal cavity and paranasal sinuses using the computational fluid dynamics method. *Eur Arch Otorhinolaryngol*. 2021;278(5):1443-1453. doi:10.1007/s00405-020-06428-3
18. Basu S, Holbrook LT, Kudlaty K, et al. Numerical evaluation of spray position for improved nasal drug delivery. *Sci Rep*. 2020;10(1):10568. doi:10.1038/s41598-020-66716-0
19. Tryggvason G. Chapter 6 – Computational fluid dynamics. In: Kundu PK, Cohen IM, Dowling DR, eds. *Fluid Mechanics*. 6th ed. Academic Press; 2016:227-291. doi:10.1016/B978-0-12-405935-1.00006-X